Lab on a Chip

Accepted Manuscript

This is an *Accepted Manuscript*, which has been through the Royal Society of Chemistry peer review process and has been accepted for publication.

Accepted Manuscripts are published online shortly after acceptance, before technical editing, formatting and proof reading. Using this free service, authors can make their results available to the community, in citable form, before we publish the edited article. We will replace this *Accepted Manuscript* with the edited and formatted *Advance Article* as soon as it is available.

You can find more information about *Accepted Manuscripts* in the **Information for Authors**.

Please note that technical editing may introduce minor changes to the text and/or graphics, which may alter content. The journal's standard **Terms & Conditions** and the **Ethical guidelines** still apply. In no event shall the Royal Society of Chemistry be held responsible for any errors or omissions in this *Accepted Manuscript* or any consequences arising from the use of any information it contains.

20 parole

Femtosecond laser fabricated microfluidic module for 3D hydrodynamic focusing allows confining fluids to a tight area in the channel center.

Figura
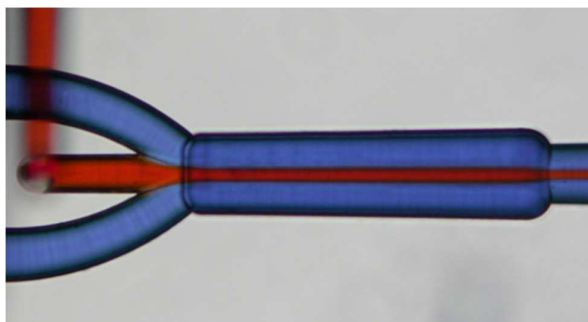
Straightforward 3D hydrodynamic focusing in femtosecond laser fabricated microfluidic channels

Petra Paiè,[a] **Francesca Bragheri,**[b] **Rebeca Martinez Vazquez,**[b] **and Roberto Osellame**[*ab]

We report on the use of femtosecond laser irradiation followed by chemical etching as a microfabrication tool for innovative microfluidic networks that implement hydrodynamic focusing. The capability of our microfabrication technology to interconnect microchannels in three dimensions is exploited to demonstrate 2D hydrodynamic focusing, either in the horizontal or in the vertical plane, and full 3D hydrodynamic focusing. In all cases only two inlets are required, one for the sample and one for the sheath flows. Fluidic characterization of all devices is provided. In addition, taking advantage of the possibility to write optical waveguides with the same technology, a monolithic cell counter based on 3D hydrodynamic focusing and integrated optical detection is validated. Counting rates up to 5000 cells/sec are achieved in this very compact device, where focusing and counting operations are implemented in less than 1 mm^3. Integration of this hydrodynamic focusing module in several devices fabricated by the same technology as optical cell stretchers and cell sorters is envisaged.

1 Introduction

Hydrodynamic focusing is a key functionality in several microfluidic devices that becomes essential when dealing with single particles, e.g. single cells in a flow cytometer, since it provides one element at a time in the detection region[1]. This would require having channels as small as the particle size (typically in the order of a few micrometers) posing severe difficulties to the microfabrication processes and significantly increasing the risk of clogging the channels. By exploiting the laminarity of the flow in a microfluidic channel, hydrodynamic focusing can be implemented, with the aid of sheath flows of buffer liquids, to confine the sample to micrometer-sized portions of a microchannel that has fractions of millimeter size[2]. This approach greatly reduces the channel clogging risk and allows a dynamic tailoring of the portion of the channel where the sample is actually flowing (Fig. 1a). Hydrodynamic focusing in microfluidic chips is mostly implemented in 2D[2–4], i.e. the sheath flow focuses the sample in only one direction, typically the horizontal one. This is accomplished by adding two additional inlets for a buffer liquid besides the inlet for the sample. The three microchannels are combined into one, and this produces a confinement of the sample by means of the sheath flow on the two sides. 2D hydrodynamic focusing, however, solves the problem only partially since particles can still overlap in

the other direction. A complete focusing of the sample into a small fluid filament can be achieved by 3D hydrodynamic focusing. This is more complicated to achieve and only few approaches have been proposed and demonstrated so far. Golden et al.[5] introduced chevron shaped grooves on the top and bottom surfaces of the channel, however these may produce air bubbles and turbulence in the flow. Goranovich et al.[6] implemented a chimney structure for the insertion and the focusing of the sample, which is however confined on the bottom surface of the channel. Rosenauer et al.[7] made use of an additional inlet on the bottom of the channel to lift the sample in the vertical direction, nonetheless this configuration requires the control of four independent inlets. A completely different approach uses centrifugal forces to perform 3D focusing on simple and planar structures[8,9]; this approach is very sensitive to the sample flow rate, thus limiting the versatility of the device. Finally, a few examples of multi-level devices[10–14] proved to be quite efficient in the realization of 3D hydrodynamic focusing and were also tested as flow-cytometers; these approaches, however, generally require complicated and multi-step fabrication processes. Most of the limitations of the above mentioned implementations rise from the fact that the technologies employed to achieve 3D hydrodynamic focusing are intrinsically 2D. This requires a higher degree of complexity to produce a 3D functionality and limits the control on the focused flow geometry. In particular, many of the devices presented above require three or more inlets[15], provide asymmetric/elliptical profiles of the focused flow[10], and confine the focused sample close to one edge of the microchannel and not in its center[16]. In addition,

---

[a] Dipartimento di Fisica, Politecnico di Milano, Piazza Leonardo da Vinci 32, 20133 Milano, Italy. E-mail: roberto.osellame@polimi.it
[b] Istituto di Fotonica e Nanotecnologie, Consiglio Nazionale delle Ricerche (IFN-CNR), Piazza Leonardo da Vinci 32, 20133 Milano, Italy.

whenever optics is used to detect/count the particles flowing in the microchannel, an external optical system is typically used, which requires careful alignment and increases the device footprint.

A recently introduced microfabrication technology is femtosecond laser micromachining (FLM) [17,18]. This technique is capable of fabricating buried waveguides and, in combination with a chemical etching step, microfluidic channels [19]. The capability of producing both waveguides and microfludic channels in the same process opens up several possibilities in the field of optofluidics [20–24]. One of the main advantages of FLM is the capability of direct writing 3D devices. While this property has been extensively exploited for producing innovative 3D photonic circuits [25–29] it has yet found little application to 3D microfluidic networks [30,31]. 3D hydrodynamic focusing is one application where the flexibility, simplicity and design freedom of FLM can introduce several improvements. In fact the sheath flow can be easily injected from several directions, without significant complications of the fabrication process. In addition, the possibility to combine the fabrication of microfluidic networks and optical waveguides in the same platform paves the way to the demonstration of new integrated devices that require optical analysis of single particles and their precise fluidic manipulation, as well as the upgrade of optofluidic devices, already demonstrated by using FLM [32–35], with the 3D focusing functionality.

In this work we exploit FLM for a straightforward fabrication of 3D mirofluidic networks that are capable of implementing 2D hydrodynamic focusing, both in the horizontal and in the vertical plane, as well as symmetric 3D focusing by using only one easy-to-operate sheath inlet. Combination of 3D focusing with optical waveguides is implemented to realize an integrated particle counter that can count up to 5000 particles/s.

2   Materials and methods

2.1   Microfluidic channel and waveguide fabrication

FLM is a powerful technique to directly fabricate buried microchannels with a very fine control of their shape and size [36,37]. All the present devices are fabricated in fused silica by a two-step process that consists in femtosecond laser irradiation followed by a chemical etching in hydrofluoric acid that selectively removes the irradiated volume [20]. Femtosecond laser irradiation is performed by means of a commercial femtosecond laser source at 1040 nm wavelength, 1 MHz repetion rate and pulse energy up to 23 μJ (femtoRE-GEN, HIGHQlaser). The microchannel irradiation pattern is realized through a 50$\times$ microscope objective (0.6 NA) that focuses the second harmonic of the laser with a pulse energy
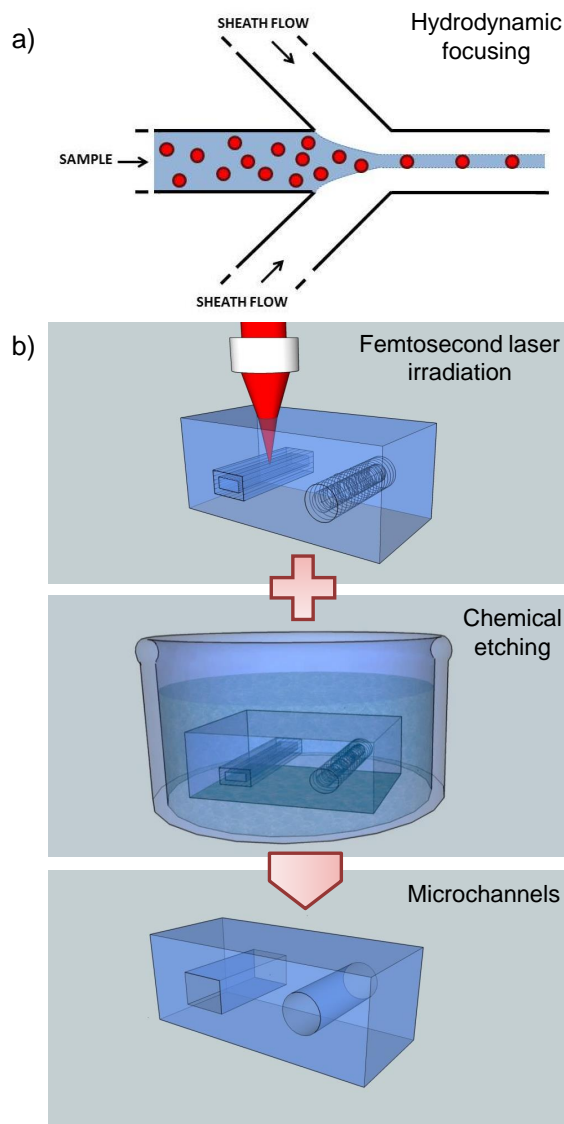

Fig. 1 a) Schematic of standard hydrodynamic focusing. Hydrodynamic focusing consists in squeezing a flow by additional side streams and in confining it to a limited portion of the microchannel. Typical implementation of hydrodynamic focusing is 2D (the central flow is squeezed to a vertical thin segment) by two side sheath flow. b) Schematic of the FLM process to produce microfluidic channels of various shapes. The glass is first irradiated by focused femtosecond laser pulses covering the surface of arbitrarily shaped cylinders. The structure is then immersed in hydrofluoric aqueous solution to selectively remove the irradiated volume and create void microchannels of controlled shape. Represented examples show microchannels with a square cross-section (used as main channel in the devices) and with circular cross section (used as access holes to connect the device to external tubing).

of 312 nJ, a scan speed of 0.2 mm/s, and an average depth below the substrate surface of 500 μm. The second fabrication step consists in a chemical etching of the irradiated structures to create the microchannels, and is performed by dipping the laser machined substrate in a 20 % aqueous solution of HF at 35°C in ultrasonic bath. The etching rate depends on the writing beam polarization[20]; therefore, during the irradiation of the microchannel pattern we have set the polarization perpendicular to the sample translation, so as to maximize the etching rate.

In order to fabricate the main channel with a square cross-section, we use a multi-scan irradiation approach: contiguous straight lines (with a separation of 2 μm) are scanned forming the surface of a rectangular cross-section cylinder. To enhance the etching rate, two cylinders are irradiated one inside the other, as can be seen in Fig.1. The size of the cross-sections of the coaxial irradiated cylinders are 50×30 μm and 85×50 μm, where the height is reduced to take into account the elongated shape of the modified volume; thanks to this compensation the microchannel after etching has a square cross-section with a $\sim$100 μm side. The curved microchannels for delivering the sheath flows and the sample to the main channel are produced by irradiating 7 parallel lines with an horizontal shift of 6 μm, leading to the formation of channels having round cross-section with $\sim$50 μm diameter. To simplify the connection of the external tubing to the microchannels, the terminations are enlarged by irradiating multiple coaxial helices with different radii (see Fig.1). In our case we irradiated 3 helices with radii of 35 μm, 70 μm and 115 μm, respectively. After the etching step, these structures become round access holes with $\sim$380 μm diameter.

In the same femtosecond laser irradiation step for the microchannel fabrication, we also directly write the optical waveguides in the device (those are not etched in the subsequent step since the irradiation conditions are different and they do not arrive to the external surface of the chip). The irradiation in the same step of both the microchannel and the waveguides is fundamental to establish a straightforward and very accurate alignment between the different components. Different waveguides across the microchannel have been fabricated at different depths, to investigate the optimal waveguide position with respect to the focused stream. This set of waveguides covered 20 μm in depth around the center of the microchannel. Although writing waveguides at different depths typically requires recalibrating the irradiation parameters due to the different influence of spherical aberrations, it was not necessary in this case due to the limited depth span. The following optical properties of the waveguides at 1 μm wavelength are obtained: propagation losses of 2 dB/cm and a mode size of $\sim$7 μm, the latter closely matching that of a single mode fiber. The waveguides writing differs from the microchannel irradiation in the following parameters: a
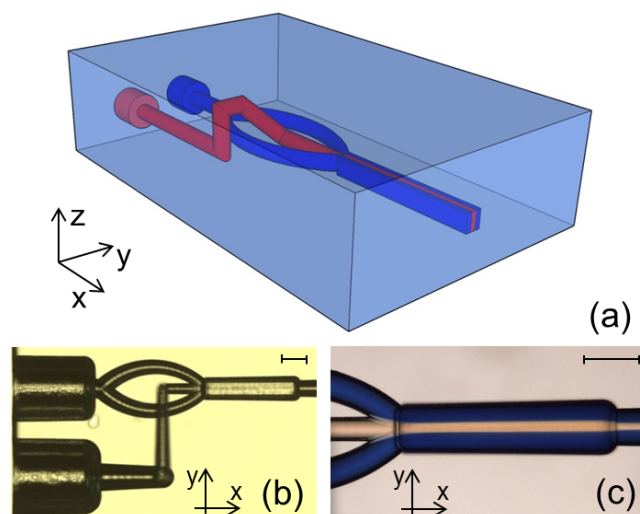
Fig. 2 2D hydrodynamic focusing in the horizontal plane. (a) Schematic rendering and (b) top-view microscope image of the fabricated device. (c) Top-view of the horizontal 2D focusing achieved with 0.7 ratio between sample and sheath flow pressures. Scale bar corresponds to 100 μm in all panels.

pulse energy of 125 nJ and a scan speed of 0.15 mm/s. No beam shaping is implemented and thus a slightly elliptical waveguide mode is observed[17,26]. Such optical waveguides are fabricated orthogonally to the main microfluidic channel; the distance between the waveguide end-faces and the channel lateral surface is 25 μm. After the chemical etching step, the sides of the fused silica chip are then polished at optical quality to improve the waveguide coupling to optical fibers; in addition, the fluidic connection of the device is achieved by PEEK tubes (of 360 μm external diameter) that are plugged into the access holes of the glass chip and glued[32,34]. It is worth emphasizing that, in this direct plug-in geometry of the tubing, the close matching of the inner cavity of the tubing with the microchannel in the chip almost eliminates dead volumes, i.e. volumes of fluids that stagnate and subtract useful sample. In fact, with the standard access holes on the top surface of the chip, the big reservoirs accumulate sample and, as a consequence, a larger amount of material than that actually measured is typically required. This is an issue when dealing with small amounts of relevant sample or when exact quantification is sought; in addition, the difficulty of cleaning these reservoirs can cause cross-contaminations between subsequent measurements in the same chip.

2.2 Device characterization

Hydrodynamic focusing was first demonstrated by monitoring the flow in the main channel using food dyes. The use of different colors for the two inlets enabled us to visualize flow confinement for the proposed 2D and 3D configurations by imaging the microchannel with an inverted Leica microscope (objective $20\times$, 0.4 NA) equipped with a CCD camera (DFC310 FX, Leica) for the bottom view, and with a separate microscope objective ($20\times$, 0.45 NA) coupled to a second CCD camera (EO-0813C, Edmund Optics) for the side view. Pressure driven pumps (Fluigent, MCFS Flex) have been used to inject and control the sample and the sheath flow in the device.

As further samples, polystyrene beads of 7 μm diameter (Sigma Aldrich) suspended in distilled water and red blood cells diluted in hypotonic solution have been used to verify the hydrodynamic focusing on microparticles. To validate the cell counting capabilities of the device proposed in Sect. 3.3, a fiber-coupled semiconductor laser at 980 nm (S26, JDS Uniphase) has been coupled to the optical waveguide that crosses the main channel at half its height, so as to match the position at which the particle flow is focused. The light transmitted through the microchannel and coupled to the waveguide on the other side (with a typical $\sim 50\%$ transmission) is collected at the output with a microscope objective and monitored by a fast photodiode (Visible DC-125 MHz, low noise Photoreceiver, New Focus). The electric signal provided by the photodiode is analysed by a sampling oscilloscope (Wavepro 735ZI, Teledyne LeCroy) to reveal perturbations in the transmitted power that indicate particles flowing through the light beam. A microscope objective was used to collect the signal out of the waveguide because the same set-up allowed us to image the particles flowing in the channel; however, a fiber could also be used on the collection side to make the device fully-integrated and alignment-free.

3 Results and discussion

The hydrodynamic focusing performances of the devices have been investigated by imaging coloured liquids and beads/cells from both top and side views. We have specifically designed and fabricated devices for implementing 2D focusing either in the horizontal and in the vertical direction, as well as full 3D focusing. In the latter device we also implemented a cell counter, taking advantage of the optical waveguides fabricated in the chip.

3.1 2D hydrodynamic focusing

A 2D hydrodynamic focusing can be implemented by squeezing the sample with two sheath flows coming from the two

sides. Renderings of the implemented layouts are reported in Fig.2(a) for the horizontal focusing and in Fig.3(a) for the vertical one. It can be appreciated that in both cases only two inlets are required, since the sheath flow is splitted from a single inlet. This is possible only thanks to the three-dimensional capabilities of this microfabrication technology. In addition, it is worth noting that, while the horizontal focusing can be achieved also with standard technologies, the purely vertical one is hardly obtained; nevertheless, the latter is quite useful when imaging the microchannel in a standard microscope set-up, in fact all the sample will be flowing on the same focal plane.

Fabrication of the fluidic network by femtosecond laser micromachining provides excellent control of the microchannel size and shape both in the horizontal (Fig.2(b)) and vertical (Fig.3(b)) configurations. In particular, the precise symmetry between the two arms of the sheath flow guarantees a balanced action of the two and thus a central position in the microchannel of the focused sample. The hydrodynamic focusing can be characterized by employing liquids with different colors for the sample and for the sheath flow (red for sample and blue for sheath flow in these 2D-focusing experiments). The amount of focusing can be controlled by the pressure ratio between the sample and the sheath flows, with an arbitrarily high confinement for a sufficiently low pressure ratio. As an example, the horizontal confinement of the sample flow to a dimension of about 20 μm is achieved with a sample/sheath pressure ratio of 0.7 (Fig.2(c)), and a similar level of vertical confinement is achieved with a pressure ratio of 0.74 (Fig.3(c)).

In both cases the sample covers the full channel size in the unfocused direction, as expected in a 2D focusing layout.

3.2 3D hydrodinamic focusing

The experimental validation with colored fluids has been performed also for the proposed three dimensional hydrodynamic focusing device. The design, which is based on the simple idea of merging the aforementioned 2D-focusing schemes, is schematically reported in Fig.4(a). Fig.4(b) and (d) respectively show the top and side view microscope images of the fabricated prototype. Since the input is composed of only two inlets, one for the sample flow and the other one dividing into four channels for the sheath flow, the hydrodynamic focusing is very easy to operate, requiring the control of only two independent pressures. In addition, the focusing functionality is achieved in a very small footprint: it covers a surface of about 1x1 mm^2.

In order to visualize the confined flow in this configuration we exploited only one colored fluid for the sample (blue in this case to increase the visibility), while transparent distilled water was used for the sheath flow. Fig.4(c) and (e) show the top and side view of the device during operation. The width of the
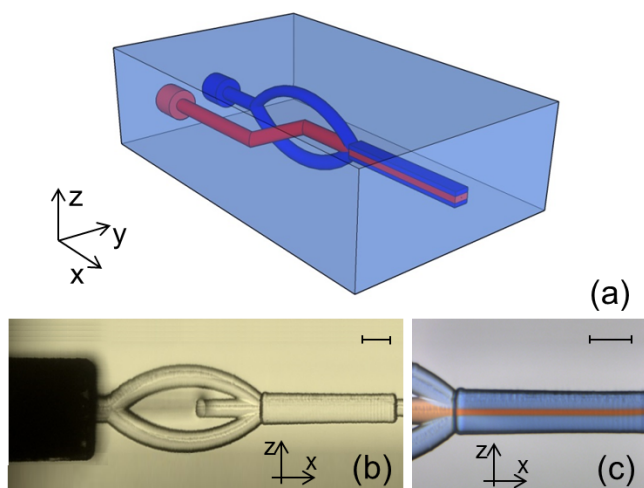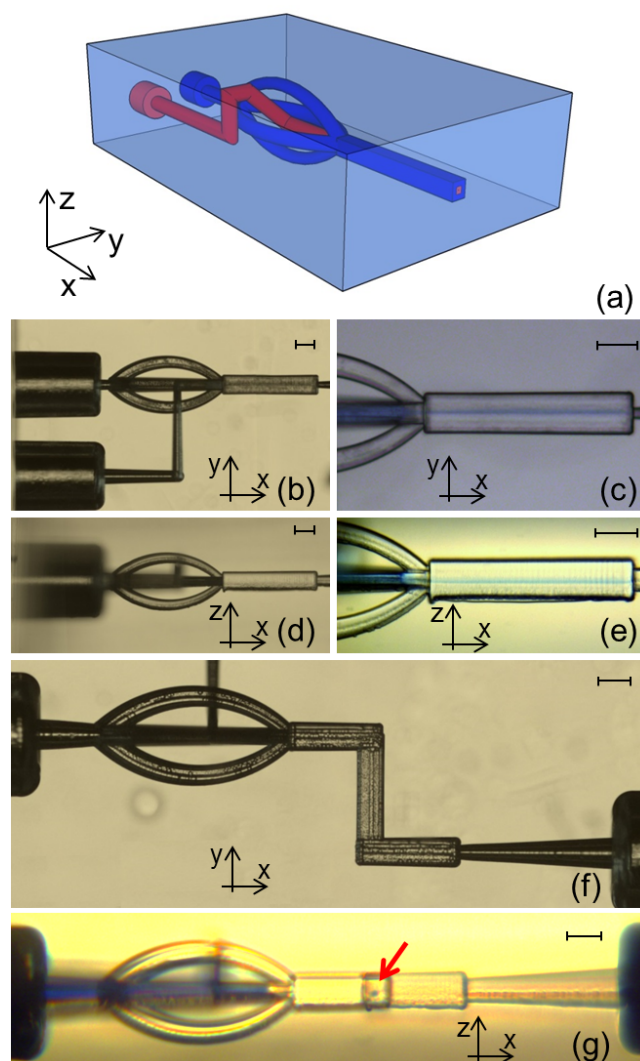
Fig. 3 2D hydrodynamic focusing in the vertical plane. (a) Schematic rendering and (b) side-view microscope image of the fabricated device. (c) Side-view of the vertical confinement achieved with 0.74 ratio between sample and sheath flow pressures. The scale bar corresponds to 100 μm in all panels.

sample flow is ~ 10 μm, both in the horizontal and vertical planes, at 0.55 sample/sheath pressure ratio. To have a better visualization of the confined flow, we have fabricated a different chip with a *Z*-shaped microchannel (top view in Fig.4(f)) after the 3D focusing section. In this way, a side imaging of the device allowed us to see the cross-section of the focused flow, which exhibited a very round profile (Fig.4(g)).

3.3 Cell/bead counter

Having demonstrated the capability of our approach to effectively focus a sample in a needle-like stream, we exploited this potentiality for the realization of an integrated cell counter. Taking advantage of the versatility of FLM, single mode optical waveguides have been fabricated in the proper depth-position, orthogonally intersecting the focused flow of sample with optical radiation. In this way, the detection of the passage of each particle is provided by a perturbation of the transmitted light. The set-up used for the cell-counting experiment is described in details in section 2.2, and is reported in Fig.5(a): a fiber-coupled semiconductor laser with an emitting wavelength of 980 nm is butt-coupled through a single mode optical fiber to a selected optical waveguide. The transmitted radiation is subsequently collected from the opposite waveguide on the other side of the microchannel, and then focused, through a microscope objective (20$\times$, 0.45 NA), on a photodiode connected to a digital oscilloscope, thus enabling to easily detect and analyze the transmitted signal. The transition of a single particle in correspondence of the

Fig. 4 3D hydrodynamic focusing. (a) Schematic rendering. (b) Top and (d) side microscope images of the fabricated device. (c) Top and (e) side view of the flow confinement in the horizontal and vertical direction achieved with a ratio between sample and sheath pressures of 0.55. (f) Top microscope image of a Z-shaped microchannel, fabricated to visualize the cross-section of the focused flow. (g) Cross section of the confined flow visualized in the Z-shaped channel from a side view. The scale bars correspond to 100 μm in all panels.

waveguide perturbs the collected signal giving rise to a net variation of the transmitted intensity. The combination of the selective illumination provided by the waveguide with the efficient 3D confinement of the sample to a size of the order of the particle dimension, assures the passage and illumination of a single particle per time in the region of interest and thus the possibility to efficiently count the number of particles in

the sample.

The validation of the device has been performed both with microspheres of polystyrene (7 μm of diameter) diluted in deionized water and with biological sample. In the latter case we prepared the sample by diluting 25 μl of blood in 1 ml of hypotonic solution. Fig.5(b) and (c) show red blood cells under the effect of 3D focusing flowing in the central region of the channel. The two images provide top and side view, respectively. It may be appreciated that Fig.5(b) also shows a whole set of optical waveguides fabricated orthogonally to the microchannel at different depths. The waveguides used for the transmission measurements are the second from the left.

A typical result of the counting experiment is reported in Fig.5(d), where it is possible to observe the presence of peaks in the signal due to the transition of cells in front of the optical waveguides. The variation in the peak amplitudes is ascribed both to the heterogeneity of the cell sample, in terms of size and shape, and to small variations of the cell heights within the focused flow. The measurements were repeated at different sample speed, keeping a constant degree of focusing (i.e. a ratio between the pressure of the sample and the sheath flow equal to 0.38). This highlights the possibility of the device to cover a wide range of velocities of the sample, ranging from few nl/min up to a maximum of 3 μl/min. In this latter case we have been able to count up to 5000 cells per second. We could not overcome this value because we reached the maximum pressure delivered by the pump system (1034 mbar). The count of the peaks has been performed by processing through a dedicated Matlab software the data registered by the oscilloscope. In particular, it was necessary to discriminate between the peaks and the noise that affects the measurement. To this end the software counts a peak as a valid signal only if its amplitude exceeds the noise level by 4 times its standard deviation, thus keeping the false-count error below the 0.006 % of the total counts. It should be noted that the detection of cells flowing in the device is based on a perturbation of the transmitted signal between the two facing waveguides. It is quite general that any kind of cell/particle, crossing the laser beam, will cause such a perturbation due to absorption, scattering, reflection and/or refraction. We therefore expect that this device will be able to effectively count particles independently of their nature and shape.

4 Conclusions

We have demonstrated a microfluidic 3D hydrodynamic focusing module that can achieve 3D symmetric flow confinement and allows confining particles to a tight area near the center of the channel. The device can be fabricated by FLM, that is a fast and rapid prototyping technique ideally suited for the fabrication of microfluidic networks with 3D geometries.

The device is easy to operate since only two inlets are needed, one for the sample flow and the other for the sheath flow that is automatically divided into four channels. The reduced size of the focusing section and the improved particle confinement in the microfluidic channel are highly desirable for integrated microfluidic flow cytometers and fluorescence activated cell sorting (FACS) or in any application where a single particle at a time is required. Here we have exploited the accurate alignment of fluidic and optical components obtained by FLM to demonstrate an integrated cell counter with rates as high as 5000 cells/s. The versatility of FLM allows one to envisage more applications and the possibility to integrate this module in already existing or newly developed more complex devices for single cell optical manipulation and analysis.

References

1 D. Huh, *Microfluidics for flow cytometric analysis of cells and particles*, Physiol. Meas. **26**, R73 (2005).

2 J. B. Knight, A. Vishwanath, J. P. Brody and R. H. Austin, *Hydrodynamic focusing on a silicon chip: mixing nanoliters in microseconds*, Phys. Rev. Lett. **80**, 3863 (1998).

3 L. Pollack, M. W. Tate, N. C. Darnton, J. B. Knight, S. M. Gruner, W. A. Eaton, and R. H. Austin, *Compactness of the denatured state of a fast-folding protein measured by submillisecond small-angle x-ray scattering*, Proc. Natl. Acad. Sci. USA **96**, 10115 (1999).

4 C. Kunstmann-Olsen, J. D. Hoyland, H.-G. Rubahn, *Influence of geometry on hydrodynamic focusing and long-range fluid behavior in PDMS microfluidic chips*, Microfluid Nanofluid **12**, 795 (2012).

5 J. P. Golden et al. *Multi-wavelength microflow cytometer using groove-generated sheath flow*, Lab Chip **9**, 1942 (2009).

6 G. Goranovic, et al. *Three-dimensional single step flow sheathing in micro cell sorters*, Modeling and Simulation of Microsystems (2001).

7 M. Rosenauer, et al. *Miniaturized flow cytometer with 3D hydrodynamic particle focusing and integrated optical elements applying silicon photodiodes*, Microfluidics and Nanofluidics **10**, 761 (2011).

8 X. Mao, J. R. Waldeisen and T. J. Huang, "*Microfluidic drifting"implementing three-dimensional hydrodynamic focusing with a single-layer planar microfluidic device*, Lab Chip **7**, 1260 (2007).

9 M. G. Lee, S. Choi and Je-Kyun Park, *Three-dimensional hydrodynamic focusing with a single sheath flow in a single-layer microfluidic device*, Lab Chip **9**, 3155 (2009).

10 Yu-Jui Chiu et al. *Universally applicable three-dimensional hydrodynamic microfluidic flow focusing* Lab Chip **13**, 1803 (2013).
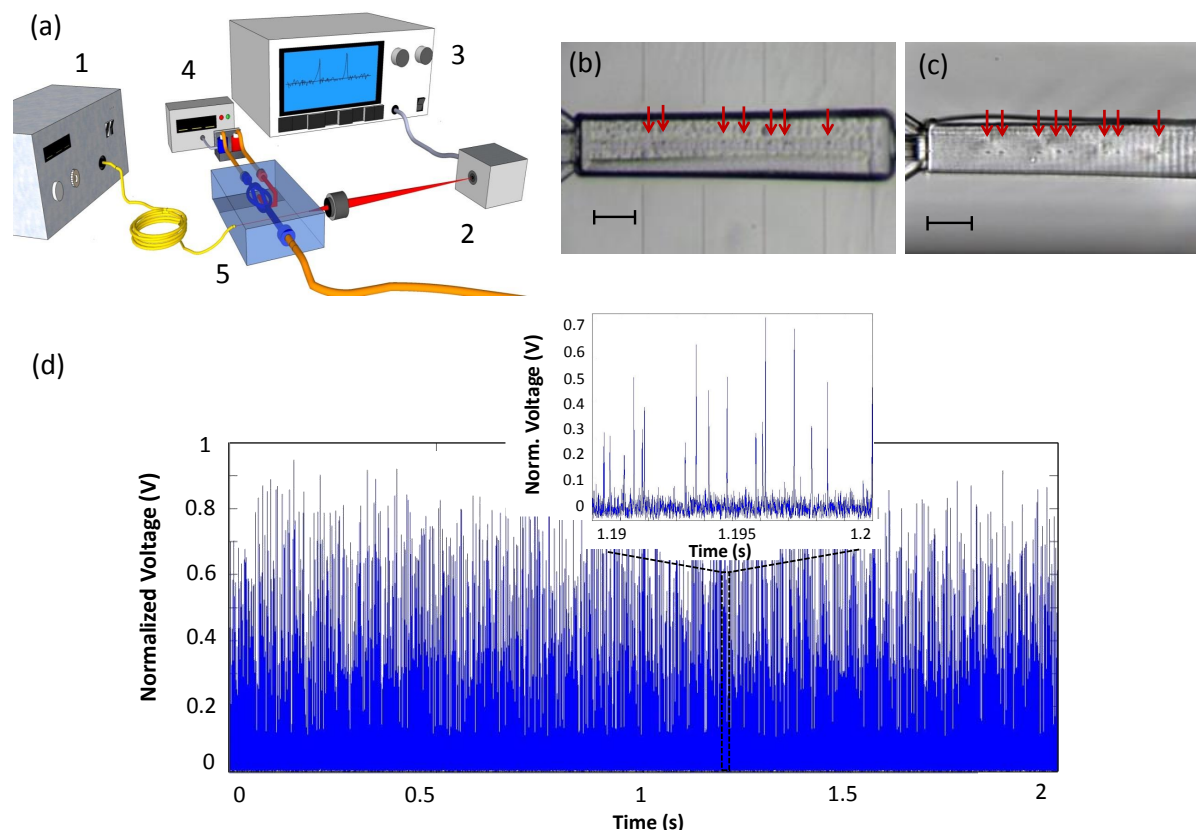
Fig. 5 (a) Schematic layout of the experimental set up: a fiber-coupled semiconductor laser (1) is butt-coupled to the waveguide in the sample; the output radiation is focused by a proper objective on a photodiode (2) which is in turn connected to a digital oscilloscope (3); pressure driven pumps (4) are used to inject and control the fluxes in the device. Top (b) and side (c) view of the device showing red blood cells flowing in a confined portion at the centre of the channel. Scale bar corresponds to 100 μm in both panels. (d) Digital oscilloscope trace of the measurement with sample/sheath pressure ratio of 0.38 and a sample speed of 3 μl/min. Each peak is related to the passage of a single cell in the region of the channel in front of the coupled waveguide, thus allowing to efficiently count the particles in the sample. The inset shows a zoomed portion of the experimental trace so as to better appreciate the single peaks.

11 R. Scott, P. Sethu and C. K. Harnett, *Three-dimensional hydrodynamic focusing in a microfluidic Coulter counter*, Review of Scientific Instruments **79**, 046104 (2008).

12 G. Zhuang, T. G. Jensen and J. P. Kutter, *Detection of unlabeled particles in the low micrometer size range using light scattering and hydrodynamic 3D focusing in a microfluidic system*, Electrophoresis **33**, 1715 (2012).

13 C. C. Chang, Z. X. Huang and R. J. Yang, *Three-dimensional hydrodynamic focusing in two-layer polydimethylsiloxane (PDMS) microchannels*, Journal of Micromechanics and Microengineering **17**, 1479 (2007).

14 M. Frankowski et al. *Microflow Cytometers with Integrated Hydrodynamic Focusing*, Sensors **13**, 4674 (2013).

15 N. Sundararajan, M. S. Pio, L. P. Lee and A. A. Berlin, *Three-dimensional hydrodynamic focusing in polydimethylsiloxane (PDMS) microchannels*, Journal of Microelectromechanical Systems, **13**, 559 (2004).

16 S. C. Lin, P. W. Yen, C. C. Peng and Y. C. Tung, *Single channel layer, single sheath-flow inlet microfluidic flow cytometer with three-dimensional hydrodynamic focusing*, Lab Chip **12**, 3135 (2012).

17 R. R. Gattass and E. Mazur, *Femtosecond laser micromachining in transparent materials*, Nature Photon. **2**, 219 (2008).

18 B. B. Xu, Y. L. Zhang, H. Xia, W. F. Dong, H. Ding and H. B. Sun, *Fabrication and multifunction integration of microfluidic chips by femtosecond laser direct writing*, Lab Chip, **13**, 1677 (2013).

19 R. Osellame, V. Maselli, R. Martinez-Vazquez, R. Ramponi and G. Cerullo, *Integration of optical waveguides and microfluidic channels both fabricated by femtosecond laser irradiation*, Appl. Phys. Lett. **90**, 231118 (2007).

20 R. Osellame, H. J. W. M. Hoekstra, G. Cerullo and M. Pollnau, *Femtosecond laser microstructuring: an enabling tool for optofluidic lab-on-chips*, Laser Photonics Rev. **5**, 442 (2011).

21 A. Schaap, T. Rohrlackb and Y. Bellouard, *Optical classification of algae species with a glass lab-on-a-chip*, Lab Chip **12**, 1527 (2012).

22 V. Maselli, J. R. Grenier, S. Ho and P. R. Herman, *Femtosecond laser written optofluidic sensor: Bragg grating waveguide evanescent probing of microfluidic channel*, Opt. Express **17**, 11719 (2009).

23 M. Kim, D. J. Hwang, H. Jeon, K. Hiromatsu and C. P. Grigoropoulos, *Single cell detection using a glass-based optofluidic device fabricated by femtosecond laser pulses*, Lab Chip **9**, 311 (2009).

24 K. Sugioka and Y. Cheng, *Femtosecond laser processing for optofluidic fabrication*, Lab Chip **12**, 3576, (2012).

25 A. Crespi, Y. Gu, B. Ngamsom, H.J.W.M. Hoekstra, C. Dongre, M. Pollnau, R. Ramponi, H. H. van den Vlekkert, P. Watts, G. Cerullo, and R. Osellame, *Three-dimensional Mach-Zehnder interferometer in a microfluidic chip for spatially-resolved label-free detection*, Lab Chip **10**, 1167 (2010).

26 S. Nolte, M. Will, J. Burghoff, and A. Tuennermann, *Femtosecond waveguide writing: a new avenue to three-dimensional integrated optics*, Appl. Phys. A **77**, 109 (2003).

27 A.M. Kowalevicz, V. Sharma, E.P. Ippen, J.G. Fujimoto, and K. Minoshima, *Three-dimensional photonic devices fabricated in glass by use of a femtosecond laser oscillator*, Opt. Lett. **30**, 1060 (2005).

28 R.R. Thomson, R.J. Harris, T.A. Birks, G. Brown, J. Allington-Smith, and J. Bland-Hawthorn, *Ultrafast laser inscription of a 121-waveguide fan-out for astrophotonics*, Opt. Lett. **37**, 2331 (2012).

29 A. Crespi, R. Osellame, R. Ramponi, D. J. Brod, E. F. Galvo, N. Spagnolo, C. Vitelli, E. Maiorino, P. Mataloni, and F. Sciarrino, *Integrated multimode interferometers with arbitrary designs for photonic boson sampling*, Nature Photonics **7**, 545 (2013).

30 Y. Liao, J. Song, E. Li, Y. Luo, Y. Shen, D. Chen, Y. Cheng, Z. Xu, K. Sugioka, and K. Midorikawa, *Rapid prototyping of three-dimensional microfluidic mixers in glass by femtosecond laser direct writing*, Lab Chip **12**, 746 (2012).

31 Y. Liao, Y. Cheng, C. Liu, J. Song, F. He, Y. Shen, D. Chen, Z. Xu, Z. Fan, X. Wei, K. Sugioka and K. Midorikawa, *Direct laser writing of sub-50 nm nanofluidic channels buried in glass for three-dimensional micro-nanofluidic integration*, Lab Chip **13**, 1626 (2013).

32 N. Bellini, K. Vishnubhatla, F. Bragheri, L. Ferrara, P. Minzioni, R. Ramponi, I. Cristiani, R. Osellame, *Femtosecond laser fabricated monolithic chip for optical trapping and stretching of single cells*, Opt. Express **18**, 4679 (2010).

33 F. Bragheri, L. Ferrara, N. Bellini, K. C. Vishnubhatla, P. Minzioni, R. Ramponi, R. Osellame and I. Cristiani, *Optofluidic chip for single cell trapping and stretching fabricated by a femtosecond laser*, J. Biophoton. **3**, 234 (2010).

34 F. Bragheri, P. Minzioni, R. Martinez Vazquez, et al. *Optofluidic integrated cell sorter fabricated by femtosecond lasers*, Lab Chip **12**, 3779 (2012).

35 N. Bellini, F. Bragheri, I. Cristiani et al. *Validation and perspectives of a femtosecond laser fabricated monolithic optical stretcher*, Biomed. Opt. Express **3**, 2658 (2012).

36 Y. Bellouard, A. Said, M. Dugan, and P. Bado, *Fabrication of high-aspect ratio, micro-fluidic channels and tunnels using femtosecond laser pulses and chemical etching*, Opt. Express **12**, 2120 (2004).

37 K. C. Vishnubhatla, N. Bellini, R. Ramponi, G. Cerullo and R. Osellame, *Shape control of microchannels fabricated in fused silica by femtosecond laser irradiation and chemical etching*, Opt. Express **17**, 8685 (2009).

Lab on a Chip Accepted Manuscript